

Seismic evaluation of Southern California embankment dam systems using finite element modeling

Mehrad Kamalzare*, Hector Marquez and Odalys Zapata

Department of Civil Engineering, California State Polytechnic University, Pomona, California, USA

(Received September 6, 2022, Revised October 25, 2022, Accepted October 31, 2022)

Abstract. Ensuring the integrity of a country's infrastructure is necessary to protect surrounding communities in case of disaster. Embankment dam systems across the US are an essential component of infrastructure, referred to as lifeline structures. Embankment dams are crucial to the survival of life and if these structures were to fail, it is imperative that states be prepared. Southern California is particularly concerned with the stability of embankment dams due to the frequent seismic activity that occurs in the state. The purpose of this study was to create a numerical model of an existing embankment dam simulated under seismic loads using previously recorded data. The embankment dam that was studied in Los Angeles, California was outfitted with accelerometers provided by the California Strong Motion Instrumentation Program that have recorded strong motion data for decades and was processed by the Center for Engineering Strong Motion Data to be used in future engineering applications. The accelerometer data was then used to verify the numerical model that was created using finite element modeling software RS2. The results from this study showed Puddingstone Dam's simulated response was consistent with that experienced during previous earthquakes and therefore validated the predicted behavior from the numerical model. The study also identified areas of weakness and instability on the dam that posed the greatest risk for its failure. Following this study, the numerical model can now be used to predict the dam's response to future earthquakes, develop plans for its remediation, and for emergency response in case of disaster.

Keywords: embankment dam; finite element modeling; levees; numerical modeling; seismic evaluation

1. Introduction

Infrastructure systems such as embankment dams and levees play a vital role in the safety of communities across the country. Embankment dams serve as reservoirs that store and hold large amounts of water for the surrounding communities and the supply is used in numerous areas of consumption including; energy production, industrial, agricultural, and urban. Levees serve as barriers for cities and communities near bodies of water and protect them against flooding. Studying the stability of these structures, the amount of forces they can withstand, and understanding the various ways it could become hazardous to human life is critical to maintaining the safety of cities established in these areas. Regardless if the cause is a man-made or natural disaster, the failure of embankment dams and levees could have catastrophic repercussions. A recent example includes the Oroville Dam Spillway failure of 2017 that was a result of a manmade error, with an independent investigation finding various organizations- including the California Department of Water Resources- at fault for hiring an under qualified engineer to design the spillway which led to the subsequent flaws in the dam, resulting in nearly \$1 billion dollars in damages and the evacuation of nearly 200,00 residents (France *et al.* 2018). A more

infamous example would be the failure of the embankment dam and levee system that occurred following Hurricane Katrina, which lead to the flooding of New Orleans and resulted in massive impacts to the economy with billions of dollars in damages and thousands of lives lost (Townsend, 2006). The examples provided illustrate that this issue does not pertain to a single area in the United States: the integrity of these infrastructure systems applies to various states across the country. As illustrated by Fig. 1, it depicts the 881 counties in the nation protected by dams and levees and more specifically, where dams and levees are located in the Los Angeles area.

Although other areas of the United States are concerned with the stability of embankment dam systems in case of hurricanes, California is concerned with their stability due to the high probability of seismic activity and the hundreds of active fault lines in the state which increase the risk of failure. Fig. 2 shows the various fault lines that are in Southern California alone, the location where this study occurred.

Determining, and subsequently studying, the failure mechanisms of embankment dams that would occur under substantial seismic loads helps the state of California be more prepared if a disaster were to occur, ultimately ensuring the safety of its citizens.

Similar studies that focus on the seismic stability and safety of dams have been conducted across the world (Nasiri *et al.* 2020). This exhibits the relevance of finding accurate methods to seismically evaluate embankment dams and potentially other structures in order to have a better

*Corresponding author, Associate Professor
E-mail: mkamalzare@cpp.edu

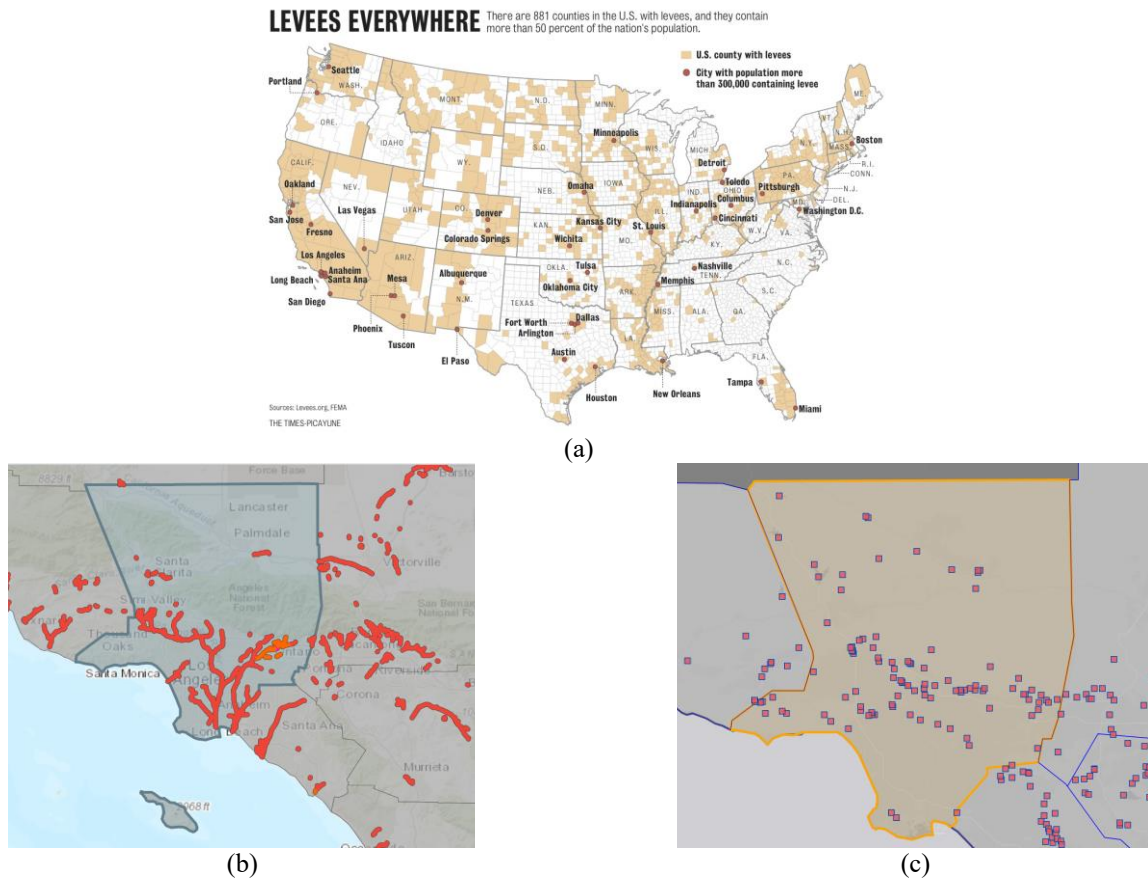


Fig. 1 Areas protected by dams and levees, (a) United States counties protected by levees, (b) Los Angeles county levees shown in red and (c) Los Angeles county dams

understanding of its response to strong motion forces and if there is anything that can be done to prepare for it. Although the methods of analysis for this particular issue require further development in order to apply it to a broader range of structures and ensure the accuracy of results, more recent studies have shown that there is progress (Babanouri and Sarfarazi 2018, Bai *et al.* 2020, Xing *et al.* 2019, Deng *et al.* 2019). An example would be the 2018 study of the Qaraoun concrete face rockfill dam in Lebanon (Almawla *et al.* 2018). This dam was chosen due to its proximity to an active fault line, specifically, being only 2.5 km away from the Yammounh fault. This dam has a greater risk for experiencing strong earthquakes, making it the ideal candidate to be evaluated. The study recognized the outdated design criteria that was used to build the dam in the 1960's- similar to the dam selected for this study- and that it needed to be updated to reflect the improvements of infrastructure safety. It would also be considered whether the dam would need to be repaired or retrofitted following this study. Using the finite element modeling software Plaxis 2D, the dam was simulated with 7.4 magnitude earthquake and a numerical model was created. It was found that the greatest settlement was experienced at the crest of the dam- similar to the results presented later in this paper- with a horizontal displacement of one meter.

Sica *et al.* (2019) conducted a study on Campolattaro Dam in Southern Italy, once again due to its close location to an active fault line. This study focused on the rapid

drawdown on the earth dam following strong seismic activity. Simulations of the earth dam's response to repeated seismic forces were created in the 2D finite difference model FLAC2D. The results highlighted an important issue that would also need to be considered for future studies if seismic evaluation of embankment dams were to continue. When experiencing repeated seismic forces, or when a seismic stage had already been experienced, analysis showed repeated seismic activity would further decrease dam stability. While the study that is discussed in this paper only conducted one simulation under different loads, Sica *et al.*'s study shows what could happen when a dam is put under continuous stress, which is a very plausible scenario during an earthquake.

Several studies that focus on seismic stability have also been conducted using different methods (Farshidfar *et al.* 2021, Fu and Wu 2019, Yamaguchi *et al.* 2018, Alonso-Estebanez *et al.* 2018, Park 2018). Zeroual *et al.* (2019) created prediction models in natural slope stability using artificial neural network (ANN) because it had the potential to provide a practical application for earth dams. In the study, four factors of safety are measured on small earth dams while they are under seismic loads or a long-term stability condition, with different computations for the two different cases being measured. A verification process was designed where predicted results were compared to those obtained from computation, and found the model predicted the factors of safety with accuracy. This is similar to the

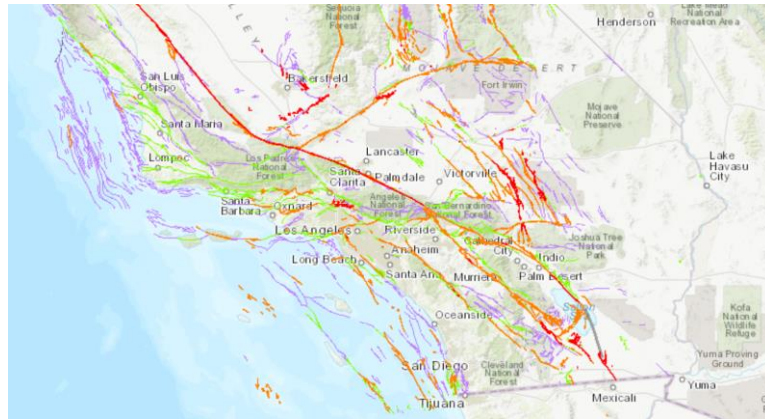


Fig. 2 Southern California fault lines

verification process that was developed for this study, which involved comparing previously recorded data to what was obtained from the simulations to determine whether the model could predict the behavior of the embankment dam accurately.

Studies have also been conducted that evaluate the seismic stability of embankment dams in regard to their materials, testing which can withstand strong motion forces. Others prefer to solely study the response embankment dams have previously had to earthquakes in order to adequately prepare as opposed to addressing issues with the dam. Regardless, finding solutions to this problem is of interest to many as embankment dams serve a vital role and are an essential piece of infrastructure. Gaining a better understanding of how these structures respond to strong seismic forces, how their composition can affect their stability, and what the most appropriate way to address such issues should be will ultimately lead to its improvement and minimizing the risk for a catastrophic disaster.

2. Research objective

The objective of this study was to create a numerical model of an existing homogeneous embankment dam using finite element modeling software, limited raw data, and resources. The embankment dam would be simulated under strong seismic forces and its results would be compared to previously recorded accelerometer data measured during similar seismic activity that was provided by the CSMIP and the CESMD. If the response of the embankment dam simulated under strong motion forces was similar to the response already recorded, it verified the model's predicted behavior. Following the verification process, it allowed the results to be analyzed in order to identify the areas that would receive the most force and therefore have the greatest risk for failure in regard to stability. The data also has the potential for future applications such as the development of appropriate emergency response plans now that the effects were clearly outlined, or developing plans to retrofit or remediate the dam to reduce the risk of its failure in case of a disaster (Kamalzare *et al.* 2016). Aside from this, the study would also develop a model for the analysis of

embankment dams that could be replicated or used in future projects that addressed the same issue.

3. Design of study

Puddingstone Dam- located in Los Angeles, California- was selected for this study. The criteria used to select a dam was; the structure needed to be equipped with accelerometers so previously recorded data would be available for the verification process, it needed to be located in Southern California, the dam had to be a homogeneous earth embankment, and it was required to have existing subsurface investigation for model parameters. Puddingstone Dam was built in 1928 and is currently operated by the Los Angeles County Flood Control District. It consists of three embankment dams- with the largest being the primary (center) dam- a concrete spillway, outlet works, and a reservoir, which has the capacity of 17,190 acre-feet and was limited to an elevation of 945 feet despite having the capacity to function at a higher water elevation. For this study, the focus will be on the main dam. The dam is a rolled earth embankment with a concrete slope protection on the upstream face, a concrete core wall to cut off seepage at the base and is drained through a triangular toe drain composed of large boulders. It has a crest height of 148 feet, crest width of 25 feet, and a crest length of 1,085 feet. Puddingstone dam is composed of locally available weathered shale bedrock, and the compacted material resulting in a sandy silty clay (CH-MH) with weathered shale fragments. Below, Fig. 3 shows the characteristics of Puddingstone Dam No. 1, as well as the cross section for the dam (Bray *et al.* 1990).

This study was created with methods previously used by Bray *et al.* (1990) and can be considered a continuation of their work. In their study, numerical models of Puddingstone Dam were created using the finite element analysis software FLUSH. Using previously recorded accelerometer data from the 1987 Whittier Narrows earthquake, Bray, et al. observed whether the simulated response to the earthquake was similar to the one recorded by accelerometers. They were essentially attempting to create a model that could accurately simulate seismic loads

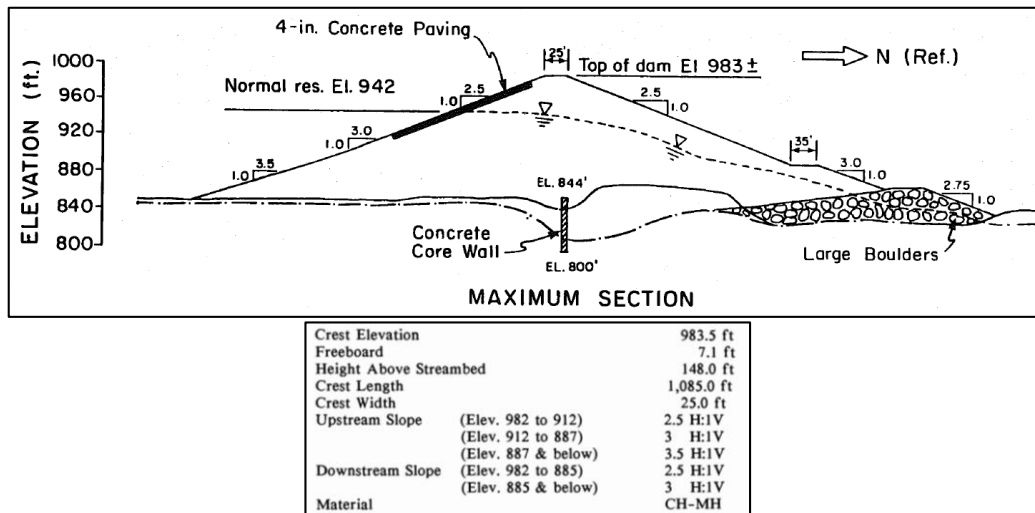


Fig. 3 Puddingstone Dam cross section and characteristics

Table 1 Strength and Stiffness Parameters used in the finite element model

		Fill (shallow)	Fill (average)	Fill (deep)	Toe Drain	Bedrock
Strength Parameters	Unit weight (pcf)	117	117	117	130	145
	ϕ (deg)	25	25	25	35	40
	c (psf)	900	900	900	0	200
Stiffness Parameters	Poisson ratio	0.4	0.4	0.4	0.35	0.4
	G_{max} (psf)	3,000,000	3,500,000	3,800,000	2,950,000	-
	γ_y	0.00065	0.00065	0.00065	0.0002	-
	a	1.5	1.5	1.5	2	-
	r	-0.75	-0.75	-0.75	-0.5	-
	E (psf)	-	-	-	-	15,000,000

onto embankment dams. In this study, the general outline for the procedures were used in order to verify that the model could still produce the desired results. However, in this case, Puddingstone Dam was modeled using strong motion accelerometer data recorded at other locations, tested to see if a similar response would occur, and used to determine areas of instability on the dam that would result in its failure.

The numerical models for this study were produced using the two-dimensional finite element modeling software RS2 (from Rocscience package). The dam was modeled based on its actual conditions that were provided in Fig. 2. Material properties based on previous subsurface investigations conducted by the International Engineering Company (IECO) in 1976. Below, Table 1 summarizes the material parameters used in this study.

The chosen material parameters were similar to those used in the 1990 study conducted by Bray *et al.* and included material types such as the embankment fill, toe drain, and bedrock abutment all measured with Mohr-Coulomb strength parameters. For material stiffness, the bedrock was modeled linear isotropically using Young's modulus (E) while other materials were modeled non-linear

isotropically using the shear modulus (G) and shear strain (γ) relationship provided in RS2.

$$G = G_{max} \left(1 + a \frac{\gamma}{\gamma_y} \right)^r \quad (1)$$

The non-linear stiffness model is presented in Eq. (1) above, and the parameters input to RS2 include the maximum shear modulus (G_{max}) and the curve fitting parameters a , γ_y , r . The embankment fill curve parameters were chosen based on those selected in the study performed by Bray *et al.* (1990). A plot of the stiffness model used for this study displaying the degradation of normalized shear modulus with increasing shear strain is presented in Fig. 4 below.

Referring once again to the study conducted by Bray *et al.* the embankment full stiffness in both studies was assumed to increase with overburden, and so it was separated into three sections; shallow, average, and deep. It should be mentioned that a strain-hardening model with non-linear stiffness would be better suited for this analysis, but it would require calibration with laboratory testing which was unavailable at the time of this study (Castelli *et al.* 2016, Elia and Rouainia 2013, Puentes *et al.* 2006,

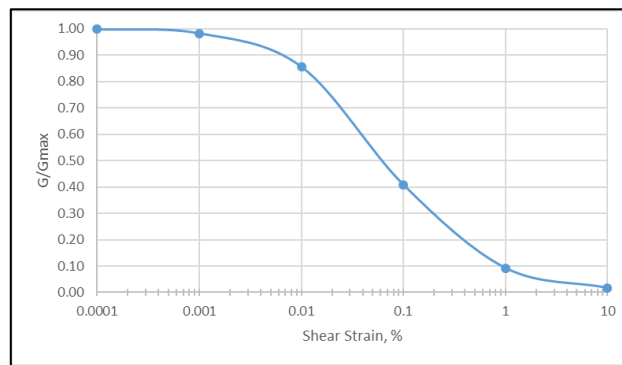


Fig. 4 Non-linear stiffness model used for embankment fill

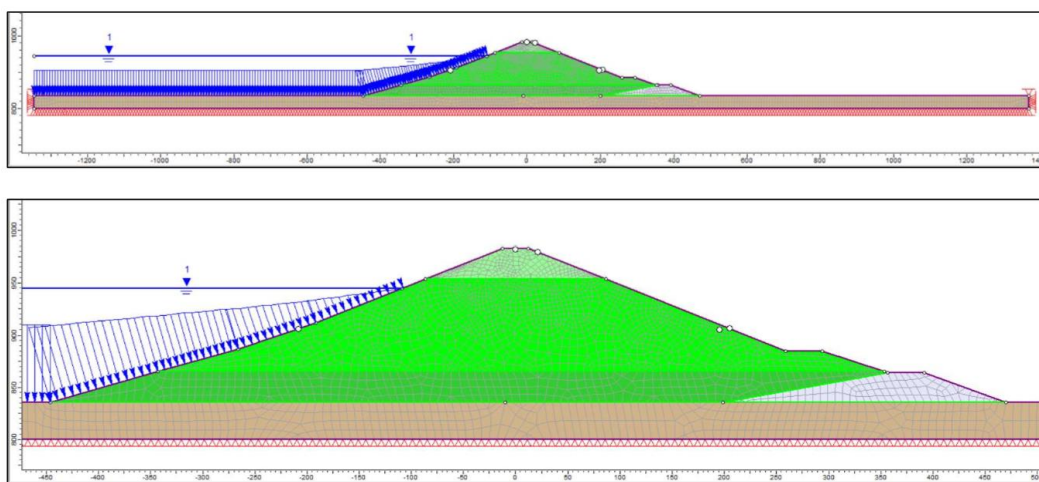


Fig. 5 RS2 model with mesh and boundary conditions

Rampello *et al.* 2009, Wu *et al.* 2009). However, the material properties that were used provided satisfactory results without the need for laboratory testing.

Analysis consisted of two stages; analyzing the model under static conditions to achieve an existing state of stress (stage 1), and dynamically where seismic motion was applied (stage 2). Each stage of analysis had its own boundary conditions. In stage 1, the ground surface was unrestrained while the lateral and base boundaries were fixed in the x and y-directions. The lateral extent was extended on both sides of the dam in order to avoid boundary condition interference with results. For stage 2, the model was entirely unrestrained but included dynamic boundary conditions where the lateral boundaries of the model were set to transmit, and the base was set to absorb incoming shear and pressure waves as if the model was unbounded.

An acceptable mesh was then applied so that all areas of the model had enough elements to obtain accurate results while limiting computing time. The actual mesh consisted of a graded mesh made up of 4 noded quadrilaterals totaling to 3,012 elements and 3,356 nodes. The mesh was generally finest at the crest and coarsest at the base. Fig. 5 illustrates the RS2 model with the above boundary and mesh conditions.

Prior to running the analysis, the strong-motion data must be properly applied. In RS2, the seismic motions are applied at the base of the model, but the strong-motion values obtained are from motions experienced at the location of the accelerometer. Therefore, the strong-motion data must be deconvoluted such that the motion input at the base of the model results in the motion recorded at the actual location of the accelerometer (ground surface/rock outcrop). In RS2, this is accomplished by taking the acceleration vs. time data and converting it to velocity vs. time, followed by dividing the velocity data by 2 and applying it as a compliant base to the model. This also led to the thickness of the bedrock layer being adjusted. Initial analyses were done with a thick bedrock layer (>100 feet) which delayed the input motion reaching the embankment fill. Therefore, the thickness of the bedrock was decreased (<50 feet) to eliminate the delay of motion. Strong motion data was then filtered to exclude data that did not provide significance to analyses-such as high frequency components- to reduce computing time.

Lastly, Rayleigh damping coefficients (α_M and β_K) were calculated for the model and used with natural frequency (ω_i) to apply a specific damping ratio to the entire model. The relationship is shown in Eq. (2).

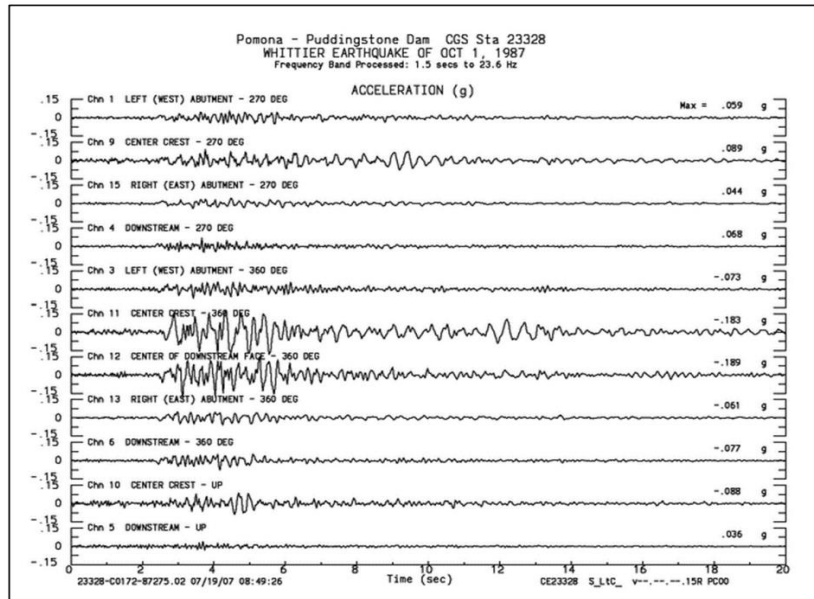


Fig. 6 Center for Engineering Strong Motion Data (CESMD) processed acceleration data output

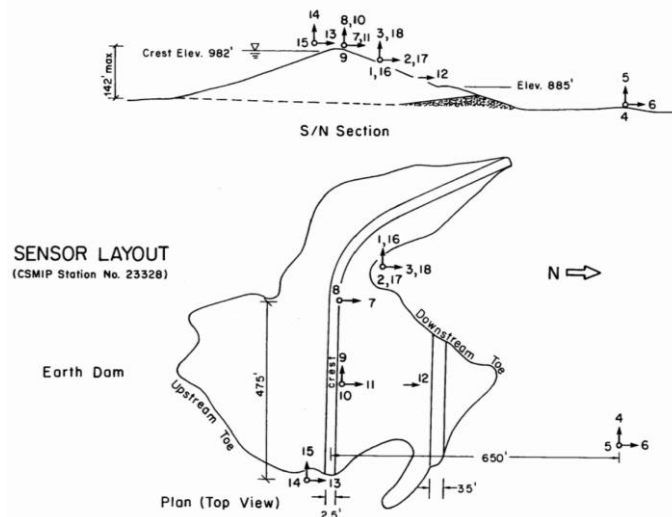


Fig. 7 Cross section and plan view with approximate location of accelerometers of Puddingstone Dam (Bray *et al.* 1990)

$$\xi_i = \frac{1}{2\omega_i} \alpha_M + \frac{\omega_i}{2} \beta_K \quad (2)$$

The Rayleigh damping coefficients were changed iteratively until the desired average damping ratio (ξ_i) was obtained. For any ratio, the damping coefficients must be updated following any changes to the model such as a change in input motion or geometry. To choose the appropriate damping ratio, an iterative process was performed during the model verification. This will be explained further in a future section of the paper.

Site specific accelerometer data was used in this study. Initial data was obtained by the California Strong Motion Instrumentation Program (CSMIP), which instrument embankment dams with accelerometers that record their

response to seismic activity. The data is then processed, corrected for baseline and sensor offset, and made public by the Center for Engineering Strong Motion Data (CESMD), providing raw and processed strong-motion data that can now be used in numerous engineering applications. Figure 6 below shows an example of processed accelerometer data at Puddingstone Dam.

Prior to running any analysis with strong-motion data on the model developed for this study, it needed to be verified with CESMD data recorded by select accelerometers on the dam in order to ensure accurate results are produced. Below, Fig. 7 illustrates a CESMD cross section and plan view of Puddingstone Dam with the approximate location of its 12 accelerometers.

For this study, only motion in the transverse (north-

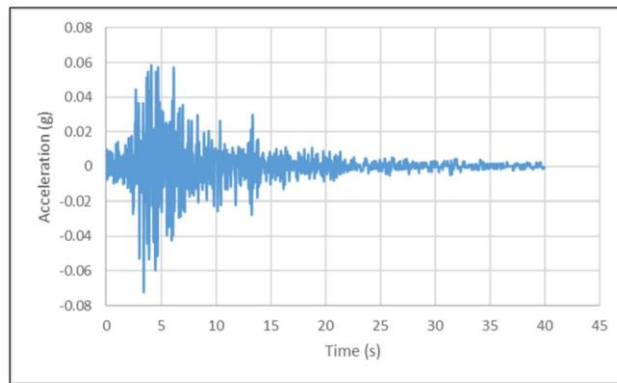
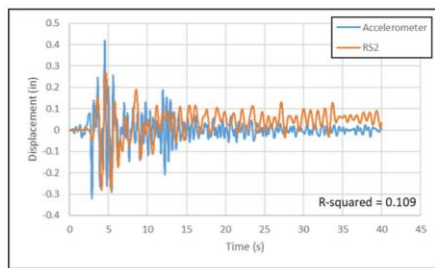
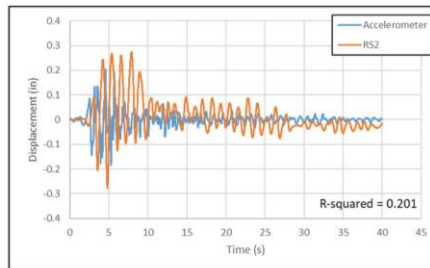


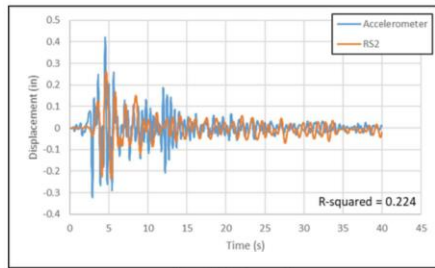
Fig. 8 Acceleration data from accelerometer 3



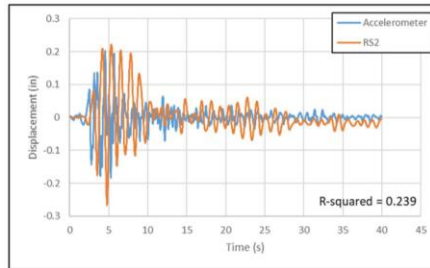
(a) 5% Damping



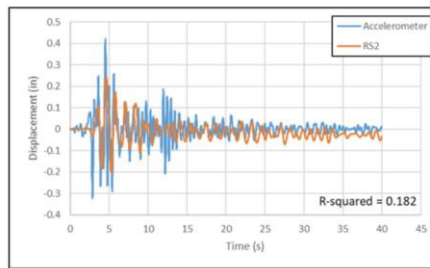
(a) 5% Damping



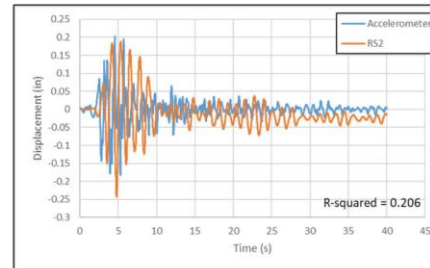
(b) 10% Damping



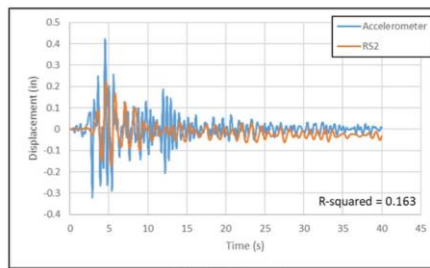
(b) 10% Damping



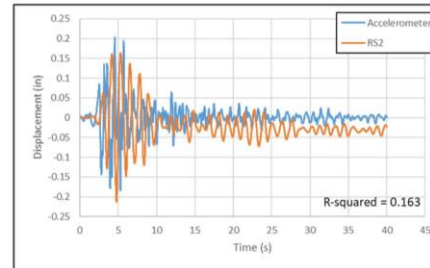
(c) 15% Damping



(c) 15% Damping



(d) 20% Damping



(d) 20% Damping

Fig. 9 Accelerometer 11 data

Fig. 10 Accelerometer 12 data

Table 2 Summary of applied strong motion data

Earthquake	Accelerometer Location	Maximum Acceleration	Rayleigh damping coefficients at 10% damping
Landers 1992 M7.3	Fire Station, Joshua Tree	0.28 g	$\alpha_M = 0.15$ $\beta_K = 0.0054$
Big Bear 1992 M6.5	Civic Center Grounds, Big Bear Lake	0.55 g	$\alpha_M = 0.17$ $\beta_K = 0.0071$
Northridge 1994 M6.4	Cedar Hill Nursery A, Tarzana	1.78 g	$\alpha_M = 0.45$ $\beta_K = 0.0044$

south) direction was analyzed and accelerometers 3, 11, and 12 were used since acceleration, velocity, and displacement data for each was readily available. Accelerometer 3 was chosen as the most appropriate for the model's input motion based on its location (ground surface/rock outcrop), and its acceleration data is shown in Fig. 8, with peak acceleration being approximately 0.07 g.

Now that the input motion and model were developed, results could be calculated. For the verification process, the model created in the study was considered verified if it produced displacement results on the dam similar to those measured by accelerometers. Accelerometers 11 and 12, located at the crest and center of the downstream face respectively, were used for model comparison purposes. As mentioned in an earlier section of the paper, the damping ratio was adjusted iteratively until the best comparison was achieved between the RS2 output and displacements from accelerometers 11 and 12. RS2 is capable of producing displacement vs. time plots at any location on the model using query points. By placing said points at the approximate locations corresponding to the location of the accelerometers, the displacement vs. time between RS2 and the accelerometers could now be compared. The data for the model needed to be corrected to begin at zero for every comparison because the displacement data produced by RS2 had displacement not equal to zero due to the static stage occurring before the dynamic stage. There also was a small difference when the RS2 results were compared to the accelerometer results. This is because the CESMD corrects accelerometer data for sensor offset while RS2 results are a direct output of the model. Regardless, comparing the direct RS2 data with the corrected accelerometer data provided resulted in an error less than 0.03 inches. The error was considered negligible for the purpose of this study. Figs. 9 and 10 demonstrate the various displacement vs. time comparisons obtained between the accelerometers and RS2 at different damping ratios.

As shown in the figure above, there is an acceptable agreement between the RS2 model and the actual accelerometer data, therefore verifying the model. Regression statistics were performed on the absolute values of the data and R-squared values to have a numerical basis of comparison between the two data sets. The computed R-square values are displayed on each graph that will be presented in a later section. The R-squared values between both accelerometers indicate the best overall agreement is obtained at 10% damping, and therefore was chosen as the damping ratio for subsequent analyses with different input motions. 10% damping was achieved with Rayleigh damping coefficients of $\alpha_M = 0.3$ and $\beta_K = 0.0077$.

4. Results

In this study, the seismic stability of Puddingstone Dam was analyzed in order to determine which areas on the dam would experience the most stress and therefore pose the greatest risk for failure. A numerical model was created using finite element modeling software and was verified using previously recorded site-specific seismic responses. The simulated behavior of the dam was then evaluated under large strong-motion data provided by the CESMD and recorded by their accelerometers. Table 2 summarizes the various input motions applied to the model, followed by their respective graphs (Fig. 11) that show the acceleration vs. time plots of each input.

The discrepancy in accelerations is a result of the location of the chosen accelerometers. Located at sites comprised of alluvium, it caused the accelerometers to experience amplified accelerations compared to nearby bedrock sites that experienced the same earthquake. This explains why Puddingstone Dam- a bedrock site- experienced much lower ground accelerations despite also being modeled to experience the same earthquake. The above motions were selected for the model because they represent strong seismic activity that frequently occurs in Southern California, and it would provide more useful results of earth embankment dams and their response to strong seismic activity that could be evaluated later on.

Displacements of the dam were measured and analyzed after the model was run with the three input motions, resulting in similar trends. Below, Table 3 summarizes the maximum displacements calculated and their locations. The sign convention is positive (+) upward/downstream and negative (-) downward/upstream. All three models resulted in having large vertical (y-direction) displacement at the crest and large horizontal (x-direction) displacement extending outwardly at the center of the downstream and upstream face.

The results of this study show the complications of the simulating any seismic behavior of embankment dams/levees. The stability of these infrastructures in the State of California, or any other place in the world where there are several active earthquake faults are among the most critical priorities. The use past earthquake response recordings should be used to address modeling challenges exist in the appropriate model development. The conducted study presented in this article shows the significance of this. Authors believe that models developed in this way can be more reliable and can help the authorities in California or other regions in the world with similar soil, and earthquake

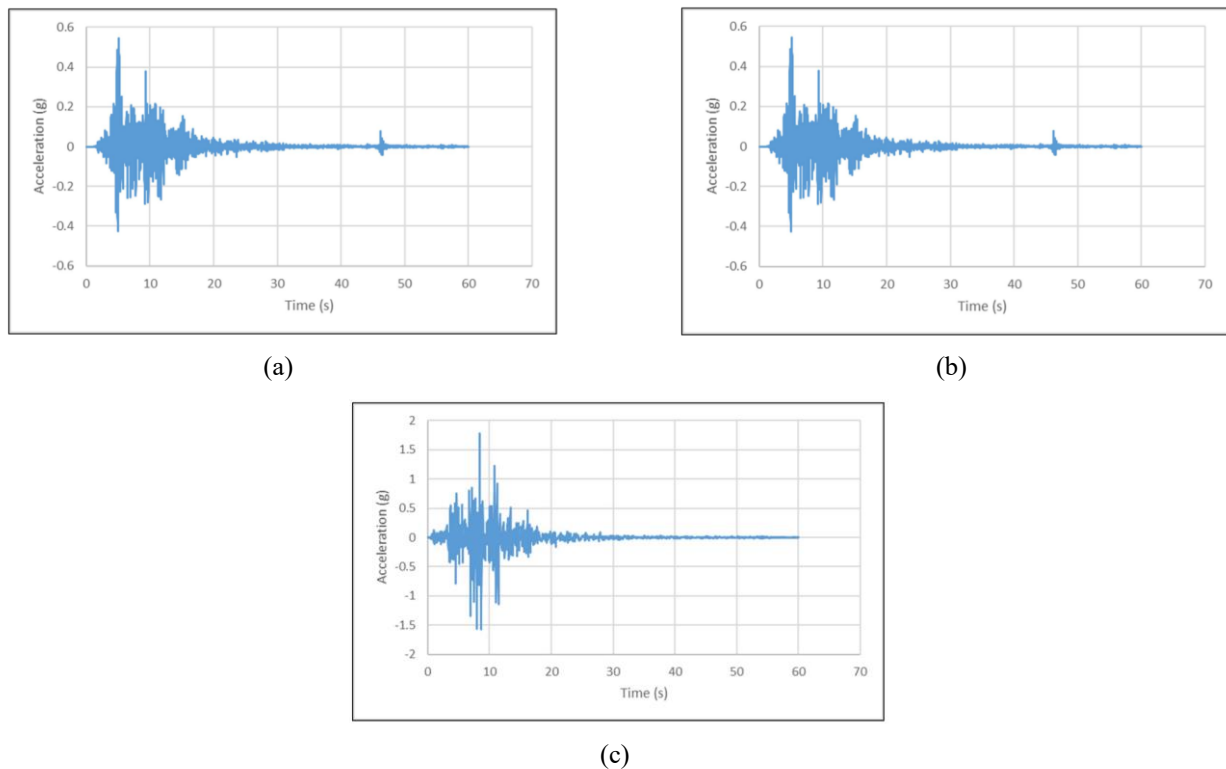


Fig. 11 Acceleration data for the considered earthquakes (a) Landers 1992, M7.3, (b) Big Bear 1992, M6.5 and (c) Northridge 1994, M6.4

Table 3 Maximum displacements summary by location

Earthquake	Crest (y-direction)	Downstream face (x-direction)	Upstream face (x-direction)
Landers 1992 M7.3	-15.6 in	+28.6 in	-27.8 in
Big Bear 1992 M6.5	-3.8 in	+4.2 in	-4.8 in
Northridge M6.4	-12.8 in	+24.6 in	-10.4 in

characteristics, to be able to model their embankment dams, and predict the zones of modes of failure due to any specific seismic loads. This can help to logistically develop appropriate maintenance program.

5. Limitations

The results of this investigation are mainly focused on the existing geology of the southern California. The findings can, however, be extended to the locations and sites with similar soil type, and general earthquake properties to southern California. Conducting seismic evaluation of dams and levees closest to fault lines using the method outlined in this study can also help to determine unstable areas and develop plans for the structure to be retrofitted, minimizing the risk of failure. It must also be mentioned that the input motions used in the numerical model were selected with the intention of easily identifying unstable areas of the embankment dam, therefore the computed results may not reflect Puddingstone Dam's

actual response during an earthquake. In order to address this issue, the dam being studied- whether it be Puddingstone or any other- must have site-specific ground motion analysis conducted to determine peak ground accelerations.

6. Conclusions

In this study, a numerical model of Puddingstone Dam simulated under strong seismic loads was developed using finite element modeling and later verified with existing accelerometer data. The numerical model specified the various failure mechanisms of embankment dams and the results highlighted the weakest areas of the dam that lacked the appropriate stability required to withstand strong motion forces. The following conclusion can be drawn from this study:

1. Puddingstone Dam's simulated response to strong-motion forces was consistent with that experienced during previous earthquakes and therefore validated the predicted behavior from the numerical model. The finite element modeling method used existing accelerometer data that illustrated the dam's response to seismic activity of a similar magnitude.
2. The predicted behavior of this study was validated using strong motion data provided by the CSMIP and processed by the CESMD. Although data already exists that recorded the deformation of the embankment dam that occurred during earthquakes of that magnitude, the numerical model

developed in this study can be used to predict the dam's response to future, and possibly stronger seismic activities.

3. Analysis showed that vertical deformation (maximum settlement) occurs at the crest of the embankment dam following strong seismic activity as a result of its underlying soil experiencing the largest amount of stress since the crest is the highest point of elevation. The study identified the crest as a particular area of concern for the stability of the dam.

4. The greatest amount of horizontal deformation is experienced halfway up the downstream and upstream slope faces, away from the center. The deformation on the dam extends as it settles.

Acknowledgements

The authors would like to thank the California State Polytechnic University, Pomona, SURE Program, and the Cypress College for their support throughout this project.

References

- Almawla, S., Fadi, H. and Kaddah, F. (2018), "Response of a lebanese rock-filled dam to seismic excitation", *WIT T. Eng. Sci.*, **121**, 33-45. <https://doi.org/10.2495/RISK180031>.
- Alonso-Estébanez, A., Del Coz Díaz, J.J., Rabanal, F., Pascual-Muñoz, P. and Nieto, P. (2018), "Numerical investigation of truck aerodynamics on several classes of infrastructures", *Wind Struct.*, **26**(1), 35-43. <https://doi.org/10.12989/was.2018.26.1.035>.
- Babanouri, N. and Sarfarazi, V., (2018), "Numerical analysis of a complex slope instability: Pseudo-wedge failure", *Geomech. Eng.*, **15**(1), 669-676. <https://doi.org/10.12989/gae.2018.15.1.669>
- Bai, T., Yang, H., Chen, X., Zhang, S. and Jin, Y., (2020). "In-situ monitoring and reliability analysis of an embankment slope with soil variability". *Geomech. Eng.*, **23**(3), 261-273. <https://doi.org/10.12989/gae.2020.23.3.261>
- Bray, J.D., Seed, R.B. and Boulanger, R.W. (1990), "Investigation of the response of Puddingstone and Cogswell Dams in the Whittier Narrows Earthquake of October 1, 1987. Volume I: Puddingstone Dam", Geotechnical Engineering Report No. UCB/GT/90-01, University of California, Berkeley, June. Also released as Data Utilization Report CSMIP/93-02, California Department of Conservation, Division of Mines and Geology, Office of Strong Motion Studies, Dec. 1993.
- California Department of Conservation (2015), "Fault Activity of California", State of California.
- Castelli, F., Lentini, V. and Trifaro, C.A. (2016), "1D seismic analysis of earth dams: the example of the Lentini site", *Procedia Eng.*, **158**, 356-361. <https://doi.org/10.1016/j.proeng.2016.08.455>.
- Deng, D., Lu, K. and Li, L., (2019), "LE analysis on unsaturated slope stability with introduction of nonlinearity of soil strength", *Geomech. Eng.*, **19**(2), 179-191. <https://doi.org/10.12989/gae.2019.19.2.179>.
- Elia, G. and Rouainia, M. (2013), "Seismic performance of earth embankment using simple and advanced numerical approaches", *J. Geotech. Geoenviron. Eng.*, **139**(7). [https://doi.org/10.1061/\(ASCE\)GT.1943-5606.0000840](https://doi.org/10.1061/(ASCE)GT.1943-5606.0000840).
- Farshidfar, N., Keshavarz, A. and Mirhosseini, S.M. (2021), "Seismic stability of reinforced soil slopes using the modified pseudo-dynamic method", *Earthq. Struct.*, **20**(5), 473-486. <https://doi.org/10.12989/eas.2021.20.5.473>.
- FEMA, and Levees.Org. (2020), "Counties with Levees", *Levees.Org*, Retrieved 5 Aug. 2020, levees.org/counties-with-levees/.
- France, J., Alvi, I.A., Dickson, P.A., Falvey, H.T., Rigbey, S. and Trojankowski, J. (2018), "Independent forensic team report Oroville Dam spillway incident", Oroville, CA, California Department of Water Resources.
- Fu, Q. and Wu, Y. (2019), "Three-dimensional finite element modelling and dynamic response analysis of track-embankment-ground system subjected to high-speed train moving loads", *Geomech. Eng.*, **19**(3), 241-254. <https://doi.org/10.12989/gae.2019.19.3.241>.
- Kamalzare, M., Zimmie, T.F., Cutler, B. and Franklin, W.R. (2016), "New visualization method to evaluate erosion quantity and pattern", *Geotech. Test. J.*, **39**(3), 431-446. <https://doi.org/10.1520/GTJ20140226>.
- Marquez, H. and Kamalzare, M. (2019), "Geotechnical risk analyses and evaluation of design criteria of embankment dam systems", *Proceedings of the 7th International Symposium on Deformation Characteristics of Geomaterials, Strathclyde's Technology & Innovation Centre*, Glasgow, UK.
- Nasiri, F., Javdanian, H. and Heidari, A. (2020), "Seismic response analysis of embankment dams under decomposed earthquakes", *Geomech. Eng.*, **21**(1), 35-51. <http://doi.org/10.12989/gae.2020.21.1.035>.
- Park, D.S. (2018), "Analyses of centrifuge modelling for artificially sensitive clay slopes", *Geomech. Eng.*, **16**(5), 513-525. <https://doi.org/10.12989/gae.2018.16.5.513>.
- Puentes, J., Rodriguez, L. and Rodriguez, A. (2006), "Numerical models for seismic response of El Buey dam", *GeoCongress*.
- Rampello, S., Cascone, E. and Grosso, N. (2009), "Evaluation of the seismic response of a homogeneous earth dam", *Soil Dyn. Earthq. Eng.*, **29**, 782-798. <https://doi.org/10.1016/j.soildyn.2008.08.006>.
- Rocscience. RS2 Tutorials. Retrieved from https://www.rocscience.com/help/rs2/tutorials/Phase2_Tutorial_s.htm
- Sica, St., Pagano, L. and Rotili, F. (2019), "Rapid drawdown on earth dam stability after a strong earthquake", *Comput. Geotech.*, **116**. <https://doi.org/10.1016/J.COMPGEO.2019.103187>.
- Townsend, F.F. (2006), *The Federal Response to Hurricane Katrina: Lessons Learned*, Retrieved from <http://library.stmarytx.edu/acadlib/edocs/katrinawh.pdf>
- Wu, C., Ni, C. and Ko, H. (2009), "Seismic response of an earth dam: finite element coupling analysis and validation from centrifuge tests", *J. Rock Mech. Geotech. Eng.*, **1**(1), 56-70. DOI: <https://doi.org/10.3724/SP.J.1235.2009.00056>
- Xing, H., Liu, L. and Luo, Y. (2019), "Water-induced changes in mechanical parameters of soil-rock mixture and their effect on talus slope stability", *Geomech. Eng.*, **18**(4), 353-362. <https://doi.org/10.12989/gae.2019.18.4.353>.
- Yamaguchi, K., Takeuchi, N. and Hamasaki, E. (2018), "Three-dimensional simplified slope stability analysis by hybrid-type penalty method", *Geomech. Eng.*, **15**(4), 947-955. <https://doi.org/10.12989/gae.2018.15.4.947>.
- Zeroual, A., Fourar, A. and Djeddou, M. (2019), "Predictive modeling of static and seismic stability of small homogeneous earth dams using artificial neural network", *Arabian J. Geosci.*, **12**(2), 1-16. <https://doi.org/10.1007/s12517-018-4162-6>.